



**HAL**  
open science

## Intra- and inter-annual changes in root endospheric microbial communities of grapevine are mainly deterministic

Marine Biget, Cendrine Mony, Tingting Wang, Ning Ling, Adèle Miteul, Olivier Jambon, Romain Causse-Védrines, Sophie Michon-Coudouel, Maxime Hervé, Véronique Chable, et al.

### ► To cite this version:

Marine Biget, Cendrine Mony, Tingting Wang, Ning Ling, Adèle Miteul, et al.. Intra- and inter-annual changes in root endospheric microbial communities of grapevine are mainly deterministic. *Plant and Soil*, 2023, 10.1007/s11104-023-06262-6 . hal-04251671

**HAL Id: hal-04251671**

**<https://univ-rennes.hal.science/hal-04251671>**

Submitted on 11 Dec 2023

**HAL** is a multi-disciplinary open access archive for the deposit and dissemination of scientific research documents, whether they are published or not. The documents may come from teaching and research institutions in France or abroad, or from public or private research centers.

L'archive ouverte pluridisciplinaire **HAL**, est destinée au dépôt et à la diffusion de documents scientifiques de niveau recherche, publiés ou non, émanant des établissements d'enseignement et de recherche français ou étrangers, des laboratoires publics ou privés.



Distributed under a Creative Commons Attribution - NonCommercial 4.0 International License

1 **Intra- and inter-annual changes in root endospheric microbial communities of**  
2 **grapevine are mainly deterministic**

3

4 Marine Biget<sup>1,2</sup>, Cendrine Mony<sup>1</sup>, Tingting Wang<sup>1,3</sup>, Ning Ling<sup>3</sup>, Adèle Miteul<sup>1,4</sup>,  
5 Olivier Jambon<sup>1</sup>, Romain Causse-Védrines<sup>1,5</sup>, Sophie Michon-Coudouel<sup>1,5</sup>, Maxime  
6 Hervé<sup>2</sup>, Véronique Chable<sup>6</sup>, Sabrina Pernet<sup>7</sup>, Philippe Vandenkoornhuys<sup>1#</sup>

7

8 <sup>1</sup> Université de Rennes 1, CNRS, UMR6553 ECOBIO (Ecosystèmes, biodiversité,  
9 évolution), F-35000 Rennes, France

10 <sup>2</sup> Université de Rennes 1, INRAE, Institut Agro, UMR IGEPP, F-35000, Rennes,  
11 France

12 <sup>3</sup> Jiangsu Provincial Key Lab for Organic Solid Waste Utilization, National Engineering  
13 Research Center for Organic-based Fertilizers, Jiangsu Collaborative Innovation Center  
14 for Solid Organic Waste Resource Utilization, Nanjing Agricultural University,  
15 Nanjing 210095, China

16 <sup>4</sup> Present address: Université Laval - Pavillon Paul Comtois - Sciences de l'Agriculture  
17 et de l'alimentation- 2425 Rue de l'Agriculture, Québec, QC G1V 0A6, Canada

18 <sup>5</sup> Université de Rennes 1, CNRS, UAR 3343 OSUR, Plateforme EcogenO, F-35000  
19 Rennes, France

20 <sup>6</sup> Institut Agro, INRAE, UMR BAGAP, 35000, Rennes, France

21 <sup>7</sup> Château Palmer, lieu dit Issan, F-33460 Margaux, France

22

23 **Running title:**

24 **root microbiota composition dynamics**

25

26 #Address correspondence to Philippe Vandenkoornhuys

27 [philippe.vandenkoornhuys@univ-rennes1.fr](mailto:philippe.vandenkoornhuys@univ-rennes1.fr)

28 UMR 6553 Ecobio, CNRS - University of Rennes 1, Avenue du General Leclerc,

29 35042 Rennes Cedex, France – Phone: +33 (0)2.23.23.50.07

30 **Abstract**

31 **Background and aims** Considering the plant microbiota, temporal changes are  
32 expected depending on plant development stages and environmental pressures because  
33 of modifications in plant requirements and available soil microbial reservoir.

34 **Methods** Herein, we analyzed the composition of root endosphere microbiota of  
35 grafted vine plants using two grapevine cultivars (Merlot and Cabernet-Sauvignon as  
36 scion grafted on rootstocks of different clones) as models both sampled in a single  
37 vineyard at three dates over a period of two growing years.

38 **Results** Highly conserved temporal patterns were found in the two cultivars. Intra-  
39 annual changes in microbial community composition were recorded whereas  
40 convergent microbial communities were observed on the two September dates. In  
41 particular, the increase in Actinobacteria and decrease in Glomeromycota in September  
42 were interpreted as shifts in the microbiota community patterns related to plant  
43 physiological requirements (e.g. water supply). A high proportion of non-random  
44 assembly of the root endospheric bacterial community confirmed the deterministic  
45 influence of the plant or/and the environment in microbial recruitment over time. The  
46 modified normalized stochasticity ratio (MST) showed that deterministic processes of  
47 assembly (MST<50%) were commonplace despite the changes in the root microbiota  
48 composition observed among sampling dates.

49 **Conclusion** Our study suggests an intra-annual rhythm of microbiota shifts, marginally  
50 random, with a succession within the root-microbiota endosphere likely governed by  
51 active plant filtering. A better knowledge of microbial-recruitment at work, seems  
52 important for both fundamental and applied perspectives.

53 **Keywords:** root microbiota, endosphere, temporal dynamics, deterministic assembly,  
54 microbiota shifts, grapevine

## 55 **Introduction**

56 Plant development and survival are largely dependent on a remarkable diversity of  
57 microorganisms (Compant et al., 2019; Lemanceau et al., 2017; Vandenkoornhuysen et  
58 al., 2015). These microorganisms, either epiphytes or endophytes, can live in all plant  
59 organs and tissues. All plants worldwide are colonized by many different types of  
60 microorganisms, the most frequently studied being bacteria and fungi (Müller et al.,  
61 2016). These plant-associated microorganisms that form plant microbiota are deeply  
62 involved in supplying the plant with water and nutrients (Trivedi et al., 2020;  
63 Vandenkoornhuysen et al., 2015). They help their host face biotic and abiotic stresses  
64 such as drought and solar radiation (Trivedi et al., 2020; Vannier et al., 2015; Yang et  
65 al., 2013). It is worth noting that microbial communities display dynamic fluctuations.  
66 In continental ecosystems, dynamic fluctuations through seasons have been evidenced  
67 and were found correlated with environmental constraints including temperature and  
68 precipitation (Liu & Howell, 2021). Deterministic processes of microbiota assembly  
69 driving changes through time can thus be hypothesized. In grafted plants, as far as we  
70 know, determinism in changes through time in the microbiota composition within their  
71 host-plant (i.e. the microbiota endosphere) has never been formally analyzed.

72 Endospheric microorganisms associated with plants originate from the environment,  
73 mostly from the soil, which thus serves as a microbial reservoir (Vandenkoornhuysen et  
74 al., 2015; Xiong et al., 2021; Zarraonaindia et al., 2015). The processes behind plant  
75 colonization shaping microbial assemblage composition are thought to be mainly  
76 deterministic, i.e. shaped by host selection (Morrison-Whittle et al., 2015; Xiong et al.,  
77 2021; and in grafted plants, Biget et al., 2023; Dries et al., 2021; Marasco et al., 2022;  
78 Vink et al., 2021). Deterministic processes are assumed to be primarily linked to plant-

79 microorganism interactions. However, randomness and neutral processes can occur  
80 (Werner & Kiers, 2015).

81 Two main mechanisms may be related to temporal fluctuations in the plant microbiota  
82 community composition. Firstly, the development stage of the plant influences plant  
83 microbiota over time (Chaparro et al., 2014; Copeland et al., 2015; Jumpponen & Jones,  
84 2010; Mougél et al., 2006). This can be explained by changes in plant needs, which  
85 thus modify the microbial assemblages recruited by the plants at the rhizosphere stage  
86 and inside the roots (Berg & Smalla, 2009; Chaparro et al., 2014). Gradual changes  
87 may also occur ranging from random colonization by species living close to the roots  
88 to preferential selection of particular species by plants (i.e. host plant preference)  
89 (Vandenkoornhuyse et al., 2002) and filtration by preferential carbon allocation to the  
90 best cooperators (i.e. deterministic changes) (Kiers et al., 2011). In addition, microbiota  
91 modifications can be linked to the development of new roots to colonize and to temporal  
92 modifications in root characteristics, shape, and functions that may modify the space  
93 available for microbial colonization (Iannucci et al., 2021; Pérez-Jaramillo et al., 2017;  
94 Saleem et al., 2018) coming together with grape phenology with, for instance, drastic  
95 changes in grape metabolism during grape ripening stage, leading to pectin and  
96 cellulose degradation, acidity decreasing, and sugars accumulation in berries (Liu &  
97 Howell, 2021; Renouf et al., 2005).

98 Secondly, environmental pressures influence plant microbiota over time. It has been  
99 empirically noticed that microbial communities vary over time, both between seasons  
100 and years (Liu & Howell, 2021; Zarraonaindia et al., 2015). In a year, climate  
101 conditions may vary strongly depending on seasons, resulting in changes in soil  
102 parameters (e.g. water availability, C/N ratio). These environmental changes over the

103 year can lead to dynamic changes in the reservoir of recruitable microorganisms, and  
104 hence in the composition of microorganisms recruited by the plant. In addition, plants  
105 respond to changes in environmental conditions and buffer abiotic stresses by recruiting  
106 particular microorganisms from the soil reservoir (Vannier et al., 2015; Vives-Peris et  
107 al., 2020). However, so far, very few studies have investigated temporal variations in  
108 plant microbiota endosphere, the most intimate fraction of the plant microbiota. We  
109 used herein grapevine as a model to assess the endospheric microbiota dynamics  
110 because grapevine has arguably a number of advantages, notably they are perennial,  
111 genetically homogeneous (i.e. herein, when made of particular scion clone grafted on a  
112 particular rootstock clone) and are usually managed very similarly at a given location  
113 and in a given vineyard domain.

114 We formulated different hypotheses. (i) The composition of both the bacteria and fungi  
115 on the grapevine varies over time. Assuming the existence of a major impact of the  
116 plant development stage as well as of modifications in the soil parameters in the  
117 different seasons, (ii) microbial differences between growing periods would be more  
118 pronounced than annual variations (same sampling date in two different years). (iii) If  
119 these temporal changes occur as a response to environmental constraints (changes in  
120 plant selection and abiotic conditions), these changes in the plant microbiota result from  
121 a combination of deterministic and stochastic processes, with the main factor driving  
122 recruitment being the soil reservoir, followed by plant-related factors (genotype/stage).  
123 To test these hypotheses, we sampled roots in a single vineyard domain located in  
124 Margaux (France). At this location, the bedrock is considered homogeneous and  
125 vineyard management is similar among fields. The root endosphere of grafted  
126 grapevine plant only have been analysed. Amplified fragment (amplicons) of fungal  
127 and bacterial small sub-unit rRNA gene obtained from root samples collected from the

128 same individual plants through time (three sampling campaigns) were sequenced to  
129 address the hypotheses.

## 130 **Materials and Methods**

### 131 **Experimental design and study site**

132 We selected individual vine plants in a single 66-ha vineyard located in Margaux,  
133 France, (45°2'12.73" N; 0°40'9.84" W). Organic and biodynamic practices have been  
134 used in the vineyard for 12 years. We sampled 25 fields (8 plant individuals per field),  
135 the number of fields containing Cabernet Sauvignon CS (12 fields) and Merlot M (13  
136 fields) clones (Fig. 1) all of similar age ranges. These two cultivars representing the  
137 upper part (scion) were grafted on rootstock 101-14 mainly. However, it can be  
138 highlighted that overall, three rootstocks types were used according to different  
139 combinations (Table S1) and M and CS rootstocks are not strictly identical. Within one  
140 plot, the plants were of the same genotype (i.e. same scion and rootstock clones). We  
141 analyzed the composition of the microbial community associated with roots of the two  
142 grapevine cultivars in September 2018 (S18), June 2019 (J19), and September 2019  
143 (S19) (June: flowering stage and September: mature grapes before harvest). The same  
144 individual grapevines were sampled in the three sampling campaigns (Fig. 1). The  
145 region is characterized by a temperate climate with average temperatures of 14.2 °C  
146 (2018) and 14 °C (2019); and cumulative annual precipitation of 934mm (2018) and  
147 1,112mm (2019). Fig. S1 shows the average daily temperature and cumulative  
148 precipitation per day recorded in the three sampling campaigns, two in 2018 and one in  
149 2019 by the DEMETER weather station located in Margaux, [http://www.meteo-](http://www.meteo-agriculture.eu)  
150 [agriculture.eu](http://www.meteo-agriculture.eu).



## 151 **Sampling and DNA extraction**

152 On each date, 200 similar non-lignified vine root fragments (i.e. roots produced during  
153 the current year) were collected to analyze variations in the grapevine root microbiota  
154 over time (25 fields x 8 plant individuals). For each individual plant, ~ 1g of healthy  
155 and non-lignified roots, of similar shape and diameter were picked close to the stem at  
156 a depth of 5-20 cm and placed in individual hermetic bags and stored in cooled packs.  
157 At the laboratory, the roots were thoroughly washed in tap water, then immersed in a  
158 5‰ Triton X100 solution for 10 minutes and finally thoroughly rinsed several times  
159 using sterile ultra-pure water (Lê Van et al., 2017). The washed roots were placed in  
160 sterile micro-tubes and stored at -80 °C until DNA processing. A representative healthy  
161 rootlet sub-sample (100 mg) of the cleaned roots was used for the DNA extraction.  
162 Total root DNA was extracted and quantified at the GENTYANE platform (Clermont-  
163 Ferrand, France) using magnetic bead technology (Sbeadex) on an Oktopure LGC  
164 Genomics automat with Hoechst 33258 reagent. The DNA samples were then stored at  
165 -20 °C until amplicon production.

## 166 **Molecular biology and sequencing**

167 All 600 extracted DNA were normalized at 10ng/μL to ensure PCR amplifications were  
168 the same for all the samples. Endospheric fungi were targeted by amplifying an 18S  
169 rRNA gene fragment with fungal primers NS22b (5'-  
170 AATTAAGCAGACAAATCACT-3') and SSU817 (5'-  
171 TTAGCATGGAATAATRRAATAGGA-3'). Endophytic bacteria were analyzed by  
172 PCR amplification of a 16S rRNA gene fragment (V5-V7 region of the 16S gene) using  
173 the bacterial primers 799F (5'-AACMGGATTAGATACCCKG-3') and 1223R (5'-  
174 CCATTGTAGTACGTGTGTA-3'). The sets of primers were customized to

175 incorporate sample tags and Illumina® adaptors. To provide normalized PCR mix and  
176 avoid contamination, Illustra™PuReTaq Ready-to-go beads (GE Healthcare®) were  
177 used for both bacterial and fungal amplifications. The PCR conditions associated with  
178 the specific targets have been detailed previously (Vannier et al., 2018). The following  
179 molecular steps were performed on the EcogenO platform (Rennes, France): briefly,  
180 PCR products were purified with AMPureXP magnetic beads (Agencourt®) and  
181 quantified with a Quant-iT PicoGreen™ dsDNA Assay Kit to insure normalization of  
182 the PCR products at the same concentration. A second PCR using the Smartchip-Real  
183 Time PCR machine (Takara) performed multiplex tagging, the resulting tagged-  
184 amplicon pool was purified (AMPureXP, Agencourt®) and quantified using the Kapa  
185 Library Quantification Kit-Illumina®. The bacterial and fungal libraries were finally  
186 sequenced on an Illumina MiSeq (PE-2x250 and PE-2x300 cycles for bacterial- and  
187 fungal-amplifications respectively, with 3 sequencing runs each). As routine in  
188 amplicon sequencing at EcogenO platform, a PCR negative control passing all the steps  
189 of the library construction was included in the sequencing procedure.

#### 190 **Raw data processing and clustering**

191 Base calling was performed on the Miseq instrument with CASAVA v1.8 software  
192 (Illumina). Sequence data trimming consisted of removing primers and deleting reads  
193 containing unidentified bases using Cutadapt software. The sequences were then  
194 processed using the FROGS pipeline following the recommendations (Escudié et al.,  
195 2018). The FROGS pipeline uses SWARM as a sequence agglomeration strategy to  
196 produce “sequence clusters”.

197 Briefly, the filtering steps recommended (Escudié et al., 2018) comprised a specialized  
198 algorithm for de-noising and a chimera removal step to exclude artificial sequence

199 clusters. Further filtering enabled removal of all sequence clusters identified in fewer  
200 than three samples and with a threshold of 0.005% of reads. After taxonomic affiliations  
201 using Silva138 16S rRNA for bacteria (Quast et al., 2012) and Phymyco-DB databases  
202 for fungi (Mahé et al., 2012), a final filtering step was applied to affiliated sequence  
203 clusters (95% coverage and 95% identity (BLAST)). The amplicon sequences did not  
204 contain any plastidial or plant mitochondrial DNA sequence. Bacterial or fungal DNA  
205 only was amplified and sequenced.

206 The resulting contingency tables contained 14 765 700 reads for bacteria and 12 483  
207 626 reads for fungi. The sequenced negative control did not contain any detectable  
208 contaminating DNA. Rarefaction curves were produced using R (“vegan” package).  
209 Sequencing depths of both bacterial and fungal microbiota were sufficient to limit  
210 sequence cluster subsampling (Fig. S2). To perform statistical analysis, because the  
211 slopes of the curves tended toward a plateau (Fig. S2), we normalized the number of  
212 reads at 8 500 and 3 700 reads for the bacterial- and fungal- dataset respectively. For  
213 the bacteria, we discarded only 13 samples (13/960 samples representing 1.4%) to  
214 rarefy at 8500 reads per sample. For the fungi, we discarded 37 samples (37/960  
215 samples representing 3.85%) to rarefy at 3700 reads per sample. None of the fields were  
216 composed of less than four out of the eight samples.

217 The final matrices containing 947 bacterial and 529 fungal sequence clusters were then  
218 used for statistical analyses. We calculated sequence cluster richness using the R “vegan”  
219 package. Index calculations and statistical analyses were performed for the dominant  
220 phyla (i.e., phyla representing the most sequence clusters with a threshold set at 5% of  
221 the total sequence clusters per date at the vineyard scale for the two microbial  
222 communities).

## 223 **Statistical analyses**

224 Statistical analyses were performed using R software version 4.0.4. We analyzed the  
225 effect of the sampling date (S18, J19 and S19) on root endospheric microbiota structure  
226 with a combination of multivariate analysis, univariate models, and neutral models. We  
227 checked if the microbial communities inhabiting the two cultivars differed using RDA  
228 (Redundancy analyses; Fig. S3). RDA were performed on Hellinger distances  
229 computed from sequence cluster matrices. The cultivar effect was assessed by a  
230 permutation test (999 repetitions) using the ‘RVAideMemoire’ package (Hervé, 2020).  
231 Because there was a significant effect of the cultivar in the two taxonomic groups (Fig.  
232 S3), all the subsequent statistical analyses were conducted separately on each cultivar  
233 to test the effect of the sampling date.

### 234 *Effect of the sampling date on microbial assemblage structure*

235 Partial principal coordinate analyses (PCoAs) were performed to assess the distribution  
236 pattern of root endospheric microbiota. PCoAs were based on Hellinger distances  
237 computed from sequence cluster matrices (Legendre & Gallagher, 2001). The  
238 individual grapevine was considered as a conditional effect to account for the biological  
239 dependency of the samples. The effect of the sampling date was assessed by a  
240 permutation test applied on the first PCoA factorial axes (function envfit () in the R  
241 ‘vegan’ package, 999 permutations). Pairwise comparisons were performed in the same  
242 way, with p-values adjusted using false discovery rate correction (Benjamini &  
243 Hochberg, 1995). PCoAs were also used to assess the effect of rootstocks on the  
244 microbial composition within each cultivar. Variation partitioning analysis (VPA) was  
245 used to test the effect of rootstock and sampling time on the community composition  
246 within each cultivar. We compared the difference in the Bray-Curtis distance to

247 compare the microbial variation between intra- and inter-annual time point under  
248 different cultivars and under the combination of scion and rootstock.

249 We used Wald tests applied to linear mixed models to test whether the sampling date  
250 impacted microbial richness. We constructed all the models using the richness index as  
251 the explanatory variable, the “individual grapevine” as random effect, and the  
252 “sampling date” as fixed effect. The linear mixed models and subsequent tests were  
253 performed using the R package ‘lme4’ (Bates et al., 2014), ‘car’ (Fox & Weisberg,  
254 2018) and ‘emmeans’ (Searle et al., 1980).

### 255 *Sampling dates differences on stochastic and deterministic assemblage processes*

256 The Sloan neutral community model (NCM) was used to determine the influence of  
257 neutral processes on the bacterial and fungal community assembly inhabiting the root  
258 (Sloan et al., 2006). This neutral model predicts the relationship between sequence  
259 cluster detection frequency and their relative abundance (Burns et al., 2016;  
260 Venkataraman et al., 2015). The model predicts that species that are more abundant in  
261 the metacommunity (total source pool) are more expected to disperse and be randomly  
262 present in different sampling conditions, whereas species with low abundance are more  
263 likely to get lost due to ecological drift (Burns et al., 2016). In this study, we conducted  
264 neutral model analyses assuming the three-date metacommunity (i.e., the total dataset  
265 of a given cultivar) was the source of microbial communities. One neutral model was  
266 generated per sampling date and per taxonomic group (fungi and bacteria). The  
267 adequacy of model fitting was assessed through  $R^2$  values ( $0 < R^2 \leq 1$ ) (Sloan et al., 2006).  
268 The sequence clusters from each matrix were then separated into three classes  
269 depending on their occurrence frequency based on a 95% confidence interval of the  
270 neutral community model predictions. The 95% confidence intervals around all fitting

271 statistics were obtained by bootstrapping with 1 000 replicates. The three categories  
272 corresponded to the sequence clusters that were more frequent than expected (above  
273 class), less frequent than expected (below class), and within the confidence interval  
274 (neutral class). The model also calculated the estimate rate “m” (read as a measure of  
275 dispersal limitation) using a non-linear least squares fitting (NLS- ‘minpack.lm’  
276 package) (Elzhov et al., 2010). The m value gives the probability of dispersal  
277 substitution from the metacommunity due to random loss of species in the local  
278 community (Burns et al., 2016). Therefore, higher m values likely show less dispersal  
279 limitation. The R code used for this analysis originated from (Burns et al., 2016). We  
280 further analyzed the sequence clusters specific to each class (above, below, and neutral  
281 classes) and extracted their taxonomic affiliations to identify the main specific  
282 taxonomic patterns that define each class associated with each sampling date.

283 The modified normalized stochasticity ratio (MST) was further used to quantify the  
284 relative importance of deterministic and stochastic process in community assembly  
285 with 50% as the boundary point between more deterministic (MST<50%) and more  
286 stochastic (MST>50%) assembly (Ning et al., 2019). The MST value was calculated  
287 based on the Jaccard distance estimated by using “tNST” functions in ‘NST’ package  
288 (Ning et al., 2019). We divided all the samples into three time points to test the influence  
289 of time series on the balance between determinism and stochasticity, and also divided  
290 them into combinations of scion and rootstock.

## 291 **Results**

### 292 **Description of the microbial composition of root endosphere**

293 The Cabernet Sauvignon (CS) matrices contained 945 (12 fields, 288 samples) and 523  
294 (12 fields, 278 samples) bacterial and fungal sequence clusters respectively while the  
295 Merlot (M) matrices contained 943 (13 fields, 307 samples) bacterial sequence clusters  
296 and 519 (13 fields, 519 samples) fungal sequence clusters.

### 297 **Effect of the sampling date on microbial community composition and richness**

298 The effect of sampling date on microbial community composition was analyzed  
299 through PCoA. PCoA analyses demonstrated clear differences in both bacterial and  
300 fungal communities among sampling dates, whatever the cultivar ( $p < 0.001$ ; Fig. 2).

301 The effect of the sampling date explained 44.2% and 41.6% ( $R^2$  in Fig. 2A, B) of the  
302 variance of the bacterial community and 25.2% and 26.9% of the variance of the fungal  
303 community ( $R^2$  in Fig. 2C, D) in Cabernet Sauvignon and Merlot respectively.

304 Regarding communities composition, J19 and S19 displayed the highest dissimilarity  
305 (Bray-Curtis distance) difference, while S18 and S19 presented the lowest difference,  
306 with similar ranges for all bacterial and fungal communities of both cultivars ( $p < 0.05$ ,  
307 Fig. S4; Fig. S5). The richness of the fungal microbiota (“all fungi”) was mainly  
308 explained by Ascomycota (the most numerous in terms of richness), and richness was  
309 lowest in J19 for both cultivars compared to S18 and S19. Reciprocally,  
310 Glomeromycota richness was significantly higher in J19 for both cultivars (Fig. 3C, D)  
311 while Basidiomycota richness had the same pattern for Merlot cultivar only. In contrast  
312 to fungi, bacteria showed no clear pattern of variation among sampling dates, except  
313 for Actinobacteria (lowest richness in J19 whatever the cultivar; Fig. 3A, B).

314 Gammaproteobacteria, Bacteroidota and Myxococcota were richer in J19 than in S18  
315 and S19 but only in the Merlot cultivar (Fig. 3B).

316 **Effect of sampling date on the stochastic and deterministic assemblages of the**  
317 **microbial communities**

318 To decipher the stochastic and deterministic processes in shaping microbial  
319 communities depending on the sampling date, we conducted neutral community model  
320 analyses (NCM) (Fig. 4A, B). Overall, the occurrence frequency of bacteria analyses  
321 was partly defined by the neutral model ( $R^2=35.5\sim43.9$  for Cabernet Sauvignon and  
322  $R^2=29.5\sim44.1$  for Merlot; Fig. 4A, B). However, for the fungal taxa, we did not record  
323 a proper fit to the model (negative  $R^2$  values Fig. S6A, B) for three out of the six models.  
324 Proper fits were found only for the J19 and S19 analyses ( $R^2=14.8$  and  $R^2=6.14$ ; Fig.  
325 S6A) and the J19 community analyses ( $R^2=15.5$ ; Fig. S6B) for Cabernet Sauvignon  
326 and Merlot, respectively.

327 In the two grapevine cultivars and on all three sampling dates, some sequence clusters  
328 of bacterial taxa occurred more frequently (10.7 to 53.9%, yellow dots) or less  
329 frequently (30.1 to 42%, green dots) than predicted by the neutral models (Fig. 4A, B,  
330 single bar charts). The yellow sequence clusters suggest active selection and  
331 maintenance by the host plant while the green taxa suggest active selection against the  
332 host (Fig. 4A, B). The stochastic fraction accounted for from 13.6 to 56.9% of  
333 cumulative microbial occurrence, thereby rejecting the null hypothesis of random  
334 assembly of the plant microbiota (hypothesis 4) (Fig. 4A, B, single bar charts).

335 Community composition defining the three classes (above, below and neutral partitions)  
336 was not evenly distributed among phyla (Fig. 4A, B, combined bar charts). Clear  
337 differences were observed for Alphaproteobacteria, Gammaproteobacteria, Bacteroidia



338 as well as Actinobacteria between the two deterministic partitions (Fig. 4A, B, “above”  
339 and “below” in the combined bar charts) indicating that within a taxonomic group some  
340 sequence clusters were deterministically selected and maintained by the host plant  
341 while others were negatively influenced by the host plant or by the local environment  
342 (Fig. 4A, B, “above” and “below” in bar charts).

343 To further quantify the relative importance of deterministic processes in shaping plant  
344 associated microbiota, and to complement the NCM analyses, the modified normalized  
345 stochastic ratio showed that MST value of bacterial and fungal communities was below  
346 the 50% boundary point, i.e. deterministic processes of assembly played a preponderant  
347 role in both bacterial and fungal communities composition in the vine root endosphere  
348 (Fig. 5; Fig. S7). The estimated minimum proportion of determinism in the community  
349 composition of endospheric microbial communities was 53% in S19 bacterial  
350 community of Merlot. MST values depended on sampling date with higher values for  
351 J19 compared to S18 and S19 for fungi; and increasing values across sampling dates  
352 for bacteria.

## 353 **Discussion**

### 354 **Composition of the grapevine root endosphere**

355 In this study, we analyzed the bacterial and fungal communities inhabiting the root  
356 endosphere and deciphered the temporal dynamics that structure microbial  
357 communities at the level of a vineyard. Proteobacteria (Alphaproteobacteria and  
358 Gammaproteobacteria) and Ascomycota were the main phyla forming the root  
359 endospheric microbiota in the grapevines in line with the results of most studies that  
360 analyzed grapevine microbial communities in different compartments, areas and  
361 climate (Bettenfeld et al., 2022). Although the microbial composition of the main phyla

362 remained stable and was similar to that described in most microbial studies of grapevine  
363 (Deyett et al., 2020; Swift et al., 2021), we observed specific changes in phyla  
364 abundances depending on the sampling date.

365 **Intra- versus inter-annual variations affect both microbial composition and**  
366 **richness**

367 In this present study, as expected, we observed consistent changes in the microbial  
368 communities of the grapevine roots depending on the sampling date, with changes in  
369 the composition, richness and selection of specific taxa (hypothesis 1). In both cultivars,  
370 we showed that intra-annual variations in the composition of microbial communities in  
371 the same year (June 2019 and September 2019) were stronger than those observed in a  
372 given growing period in two different years (September 2018 and September 2019)  
373 (hypothesis 2). Similarly, but in a different compartment, the rhizosphere, a recent study  
374 showed changes in the bacterial and fungal richness of grapevine related to the sampling  
375 date during the year (Berlanas et al., 2019). Elsewhere, in grafted grapevine, it has been  
376 shown that the combination of both scion and rootstock determine, at least in part, the  
377 root microbiota composition (Marasco et al., 2022) with a more pronounced effect of  
378 rootstock as driver of the deterministic process of assembly of the grapevine root  
379 microbiota (Biget et al., 2023). Considering the observed changes in the grapevine root  
380 microbiota composition through time, we noticed that (i) almost all scion and rootstock  
381 combinations showed less variation within than between years (Fig. S5) (ii) the  
382 assembly process considering the different time points under almost all combinations  
383 of rootstock and scion is deterministic (Fig S7) which is not coherent with the  
384 observation (i.e. less variation between years) despite a confirmed effect of the  
385 rootstock type on the microbial composition (Fig S8 and S9). Taken altogether, and

386 despite the limits of these analyses of the rootstock effect (i.e. redundancy between  
387 factors field and rootstock-scion combination), the results (Figs S5-S9) suggest that the  
388 changes observed among sampling dates in the grapevine root endosphere microbiota  
389 composition are not a consequence of divergences related to the rootstock type but  
390 rather seemingly convergent response patterns related to external effector.

391 Regarding the composition of the bacterial community, we particularly observed that  
392 Actinobacteria were significantly richer in September than in June, whereas  
393 Bacteroidota and Myxococcota were richer in June. Actinobacteria have been described  
394 to improve plant mineral and hydric nutrition (Govindasamy et al., 2014) and may thus  
395 have been recruited by the plant in greater numbers in September to buffer abiotic  
396 stresses at the end of the summer. Monthly rainfall and mean temperature were 36.8  
397 mm and 20.6°C, 134.0 mm and 20.9°C, 71.0 mm and 20.0°C for Sept 18, June 19 and  
398 Sept 19 respectively. It can thus be suggested that the microbiota composition changes  
399 are related to water availability. In support to this, analyses of synchronic effect of  
400 drought on the microbiota composition have previously demonstrated changes in the  
401 plant endosphere microbiota composition (Andreo-Jimenez et al., 2019).

402 Some genera among Actinobacteria, particularly *Streptomyces*, are known to control  
403 pathogens by producing antibiotic molecules (Doubou et al., 2001; Schrey & Tarkka,  
404 2008). Thus, these *Streptomyces* can help to suppress phytopathogens and plant  
405 diseases. We detected specific *Streptomyces* sequence clusters at the two September  
406 sampling dates (the same sequence-clusters were identified in September 2018 and  
407 September 2019, Table S3). Because the critical development stage of grapevines is at  
408 the end of grape ripening, it can be suggested that the plants may secrete specific  
409 exudate compounds to recruit Actinobacteria to face both biotic and abiotic stresses.

410 The increase in Bacteroidota in June can be explained by their role in plant nutrition.  
411 Indeed, Bacteroidota have been reported to be involved in organic phosphorus  
412 mineralisation (Lidbury et al., 2021). Recruiting Bacteroidota in June, when the plants  
413 reach their highest vegetative growth phase, may help them to face increasing demand  
414 for mineral nutrition. Changes in bacterial communities between the flowering and the  
415 harvest periods (mature grapes) appeared to be in line with developmental grapevine  
416 stages, both involving differential plant needs.

417 The composition of the fungal community was also strongly influenced by the sampling  
418 date, with higher Basidiomycota (only for Merlot) and Glomeromycota richness in June  
419 and higher Ascomycota richness in September. A recent study investigated intra-annual  
420 changes in fungal communities of different bio-compartments, which supports our  
421 results on the root endosphere (Liu & Howell, 2021). They correlated weather  
422 conditions with changes in fungal composition and observed dramatic changes in  
423 microbiota composition and diversity especially at the veraison stage, just after the fruit  
424 set period (Liu & Howell, 2021). Glomeromycota forming Arbuscular Mycorrhiza (AM)  
425 are known to be involved in supplying minerals and water to plants and in improving  
426 resistance to plant diseases (Smith & Read, 2010). Thus, changes in the patterns of AM  
427 fungal community composition over time that have already been evidenced (Bennett et  
428 al., 2013; Vandenkoornhuysen et al., 2002) may be correlated with the plant  
429 development stage and plant requirements over the seasons. Beyond this aspect, the  
430 shifts in AM symbiosis composition may be partly attributable to a demonstrated  
431 priority effect (i.e. the effect of order of arrival on subsequent community development)  
432 (Werner & Kiers, 2015).

433 Many endospheric Basidiomycota and Ascomycota that form positive associations with

434 plants (i.e. endophytic fungi) are known as plant “protective agents” (Porrás-Alfaro &  
435 Bayman, 2011) that promote plant resistance to environmental stresses including  
436 drought, salinity, heat, insects, and pathogens (Hardoim et al., 2015; Porrás-Alfaro &  
437 Bayman, 2011). For instance, under drought conditions, rice has an enriched fungal  
438 endosphere that has been interpreted as positive recruitment to buffer drought  
439 conditions (Andreo-Jimenez et al., 2019). Fungal endophytes are known to induce a  
440 plant systemic resistance (ISR) while these fungal symbionts escape this immune  
441 response (Hardoim et al., 2015). In addition, it has been demonstrated *in vitro* that some  
442 of these recruited fungi are able to produce antifungal metabolites (Hardoim et al., 2015)  
443 which might modify the diversity of the root-fungal endosphere. Further analysis  
444 including an absolute quantification of each fungus composing the grapevine  
445 mycobiota might provide complementary information to reinforce conclusions related  
446 to the changes observed. More widely, the temporal changes in root-endosphere  
447 community composition over time raise the question of the extent of the determinism  
448 in the process of assembly.

#### 449 **Stochastic versus deterministic process of assembly of the grapevine root** 450 **endosphere over time**

451 Recent advances in statistical analyses have allowed to partition deterministic and  
452 ecologically neutral processes of assembly using a null model framework (Burns et al.,  
453 2016) (see Materials and Methods for the rationale). For fungi, the absence of a fit of  
454 the neutral community model (NCM) analysis did not allow partitioning with statistical  
455 support for stochastic and deterministic processes of assembly. However, considering  
456 bacteria, we were able to estimate that the deterministic part accounted for 43 to 84%  
457 for the two grapevine cultivars (Fig. 4) (hypothesis 3). This appeared consistent with

458 non-random assembly of bacterial communities inhabiting the root endosphere of  
459 grafted grapevine plants, although the grafted plants were compared to the ungrafted  
460 plants under the holobiont concept (Biget et al., 2023). In our study, we defined a new  
461 non-random assemblage process of the grafted plant along a seasonal variation. This  
462 new process seems independent from the rootstock genotype, a factor supposedly  
463 inducing variance (i.e. a random-like part of the partitioning). The endosphere  
464 composition dominated by deterministic assembly processes can be explained by active  
465 rejection of bacteria by the host (bar charts showing the cumulative occurrence  
466 frequencies of sequence clusters in Fig. 4), and to a lesser extent to sequence clusters  
467 actively maintained and selected by the host plant. Previous studies have showed that  
468 the endophytic communities in *Pinus* were structured by host age and environmental  
469 factors (Carper et al., 2018). It has been shown in plant microhabitats (roots, shoots)  
470 that deterministic processes of assembly were primarily responsible for community  
471 assembly likely related to plant filtration processes (Guo et al., 2021). The determinism  
472 governing the community assembly also suggested thinly tuned filtering processes in  
473 grapevine root-endosphere composition over time in this study. The specific selection  
474 of key taxa by the host plant can be interpreted as a process to face particular  
475 environmental conditions or to meet specific needs. Increasing evidence has explained  
476 selection and regulation of rhizospheric microbial communities through root exudates  
477 (Broeckling et al., 2008; Chaparro et al., 2013; Chaparro et al., 2014; Voges et al. 2019;  
478 Zhalnina et al., 2018). Depending on their development stage, plants can secrete  
479 different types of compounds, including specific sugars and amino acids as well as more  
480 complex secondary metabolites (Cotton et al., 2019; Jacoby et al., 2020; Voges et al.,  
481 2019), that act as signals for microbial assemblages of the rhizosphere habitat (Chaparro  
482 et al., 2014). It has been recently shown that coumarins solubilized iron under particular

483 oxygen and pH conditions thus stimulating rhizospheric microbial growth in these  
484 specific conditions (McRose et al., 2023). It is thus not only the control of carbon  
485 released by plants but also the physicochemical status which modulates the rhizosphere  
486 composition. Modifications in rhizosphere microbiota and in plant microbiota  
487 evidenced herein over time may thus be a consequence, at least partially, of both  
488 changes in the root secondary metabolites excreted (Dang et al., 2021; Kaur & Suseela,  
489 2020; Voges et al., 2019) and physicochemical modifications related to water  
490 availability. The rhizosphere being the antechamber of the endosphere, this process  
491 should act together with the plant immune system and the mechanism of preferential C  
492 allocation to the best cooperators (Kiers et al., 2011). This process would explain the  
493 determinism observed in microbiota assembly in root-endosphere samples.

#### 494 **Convergence of temporal shifts in the microorganisms root-endosphere** 495 **composition between the two cultivars**

496 A key result of this work is the convergence of the temporal dynamics of  
497 microorganisms between the two cultivars, Cabernet Sauvignon and Merlot. The  
498 rootstock genotypes used in Cabernet Sauvignon (CS) are not strictly comparable to  
499 Merlot (M) (Table S1). At least two plots contained a specific rootstock genotype  
500 associated with Merlot scion. From this and because we have recently demonstrated  
501 that rootstock is the key driver of endospheric microbiota composition (Biget et al.,  
502 2023) we expected to observe differences among grafted Cabernet Sauvignon and  
503 Merlot. Conversely to the expectation over drivers than plant material can be the  
504 observed convergence in the microbiota composition. It can be argued that the  
505 environmental conditions (lower water availability) in September might cause a  
506 convergent change in the endospheric microbiota composition. It is possible that in

507 addition to the environmental stress, the plant growth developmental stage is also  
508 important to consider. If this is true, the high convergence observed in the endospheric  
509 microbiota composition can be interpreted as empirical evidence of deterministic  
510 selection during plant growth and development. This interpretation is in agreement with  
511 recent findings in the maize microbiome, i.e. the plant developmental stage as driver of  
512 differentiation in ecological functions of the plant-microbiota and consequently of the  
513 recruited microorganisms forming this microbiota (Xiong et al., 2021).

514 The root microbiota has been characterized as a combination of dynamic processes  
515 (primary colonization of microbes from the surrounding soil followed by host  
516 recruitment) (Bulgarelli et al., 2013). Our results suggest that these mechanisms –  
517 priority effect and host preference – are likely to be similar regarding the type of the  
518 cultivar analysed and greatly expand on the development of the host plant. Although  
519 variations in microbial composition depending on cultivar type and on the genotype  
520 have been proposed, most of the work done so far acknowledged that the geographical  
521 location and local environmental conditions (climate/soil parameters) had a bigger  
522 impact on microbial assembly (Bokulich et al., 2014; Marasco et al., 2018;  
523 Zarraonaindia et al., 2015; Zhang et al., 2019). We have worked herein at the level of a  
524 vineyard domain to limit the effect of bedrock and related soils characteristics,  
525 viticulture practices and environmental conditions and confirmed differences in the  
526 microorganism endosphere community composition in between Cabernet Sauvignon  
527 and Merlot (Fig. S3) and more importantly demonstrated that the two cultivars  
528 analyzed responded temporally in the same way, i.e. same key intra- and inter-cultivar  
529 variations in the microbial-endosphere structure through time. To confirm our results,  
530 the temporal dynamics of the microbiota should now be tested on a larger number of  
531 cultivars at a given location under similar viticultural practices.



532 **Conclusion**

533 The study of microbial temporal dynamics advanced our understanding of the  
534 mechanisms governing their assemblages and demonstrated tight relationships between  
535 microbial assemblages and plant phenology and adaptation to environmental conditions.  
536 Here, we showed similar patterns between the two cultivars, both cultivars displayed a  
537 deterministic recruitment of specific microorganisms and harbour similar trend in  
538 microbial communities variation. Beyond this framework, our understanding of the  
539 mechanisms behind the deterministic changes, including the relative effect of the host  
540 plant versus abiotic conditions, remains incomplete. Our results stress the complex  
541 interactions that take place between a host and its microbiota over time. Understanding  
542 microbial assembly rules would help preserve grapevine health, and possibly will allow  
543 to understand the particularity of vintages and intensify the spirit of the wine (*microbial*  
544 *terroir*). However, fundamental research is still needed to understand the mechanisms  
545 of microorganisms recruitment and dynamics in the endosphere. One promising  
546 prospect would be to analyse in gnotobiotic conditions (i.e. with the use of a culture  
547 collection) how plants attract specific microorganisms (e.g. dynamic analyses of  
548 exudates composition emitted) and also to better decipher the importance of source-  
549 sink transitions for carbon in relation to the developmental stage of the plants.

550 **Acknowledgements**

551 This work was supported by a grant from the CNRS-EC2CO program (HOLOBIONT  
552 project), CNRS-IRP program (M-AGRI project) and by the "*Agence Nationale de la*  
553 *Recherche et de la Technologie*" (ANRT) through an industrial CIFRE agreement  
554 between Château Palmer, Château Latour, Sovivins, Pépinière de Salettes and the  
555 University of Rennes 1 (Agreement N° 2017/1579). We are grateful to the  
556 GENTYANE and, within the ANAEE-France research infrastructure, to the EcogenO  
557 platforms for help with DNA extraction and amplicon sequencing, respectively. We are  
558 also grateful to the Genotoul platform Toulouse Midi-Pyrenees and GenOuest for  
559 access to their bioinformatics pipeline and storage facilities and the Ecolex platform for  
560 help during sampling. We deeply acknowledge all the trainees and people at Château  
561 Palmer for their help during the sampling campaigns, especially Sylvain Fries, Oriane  
562 Heulliet, Hélène Sarkis for their help performing this work. We are also very grateful  
563 to July Hémon (EcogenO, molecular analysis) and Achim Quaiser (sampling). We  
564 finally acknowledge Daphne Goodfellow for English editing.

565 **References**

- 566 Andreo-Jimenez, B., Vandenkoornhuysen, P., Lê Van, A., Heutinck, A., Duhamel, M.,  
567 Kadam, N., Jagadish, K., Ruyter-Spira, C., & Bouwmeester, H (2019) Plant host and  
568 drought shape the root associated fungal microbiota in rice. *Peer J* 7: e7463.  
569 <https://doi.org/10.7717/peerj.7463>
- 570 Bates, D., Mächler, M., Bolker, B., & Walker, S (2014) Fitting linear mixed-effects  
571 models using lme4. *J Stat Softw* 67:201-210. <https://doi.org/10.18637/jss.v067.i01>
- 572 Benjamini, Y., & Hochberg, Y (1995) Controlling the false discovery rate: a practical  
573 and powerful approach to multiple testing. *J R Stat Soc* 57:289-300.  
574 <https://doi.org/10.1111/j.2517-6161.1995.tb02031.x>
- 575 Bennett, A. E., Daniell, T. J., Öpik, M., Davison, J., Moora, M., Zobel, M., Selosse,  
576 M.-A., Evans, D (2013) Arbuscular mycorrhizal fungal networks vary throughout the  
577 growing season and between successional stages. *PloS One* 8:e83241.  
578 <https://doi.org/10.1371/journal.pone.0083241>
- 579 Berg, G., & Smalla, K (2009) Plant species and soil type cooperatively shape the  
580 structure and function of microbial communities in the rhizosphere. *FEMS Microbiol*  
581 *Ecol* 68:1–13. <https://doi.org/10.1111/j.1574-6941.2009.00654.x>
- 582 Berlanas, C., Berbegal, M., Elena, G., Laidani, M., Cibriain, JF., Sagües, A., Gramaje,  
583 D (2019) The fungal and bacterial rhizosphere microbiome associated with grapevine  
584 rootstock genotypes in mature and young vineyards. *Front Microbiol* 10:1142.  
585 <https://doi.org/10.3389/fmicb.2019.01142>
- 586 Bettenfeld, P., Cadena i Canals, J., Jacquens, L., Fernandez, O., Fontaine, F., van  
587 Schaik, E., Courty, P.-E., & Trouvelot, S (2022) The microbiota of the grapevine  
588 holobiont: A key component of plant health. *J Adv Res* 40:1-15.  
589 <https://doi.org/10.1016/j.jare.2021.12.008>
- 590 Biget, M., Wang, T., Mony, C, Xu, Q., Lecoq, L., Chable, V., Theis, K.R., Ling, N.,  
591 Vandenkoornhuysen, P (2023) Evaluating the hologenome concept by analyzing the  
592 root-endosphere microbiota of chimeric plants. *iScience* 26:106031.  
593 <https://doi.org/10.1016/j.isci.2023.106031>
- 594 Bokulich, N. A., Thorngate, J. H., Richardson, P. M., & Mills, D. A (2014) Microbial  
595 biogeography of wine grapes is conditioned by cultivar, vintage, and climate. *Proc Natl*  
596 *Acad Sci USA* 111: E139-E148. <https://doi.org/10.1073/pnas.1317377110>
- 597 Broeckling, C. D., Broz, A. K., Bergelson, J., Manter, D. K., & Vivanco, J. M (2008)  
598 Root exudates regulate soil fungal community composition and diversity. *Appl Environ*  
599 *Microbiol* 74:738-744. <https://doi.org/10.1128/AEM.02188-07>
- 600 Bulgarelli, D., Schlaeppi, K., Spaepen, S., Van Themaat, E. V. L., & Schulze-Lefert, P  
601 (2013) Structure and functions of the bacterial microbiota of plants. *Annu Rev Plant*  
602 *Biol* 64:807-838. <https://doi.org/10.1146/annurev-arplant-050312-120106>
- 603 Burns, A. R., Stephens, W. Z., Stagaman, K., Wong, S., Rawls, J. F., Guillemin, K., &  
604 Bohannan, B. J. M (2016) Contribution of neutral processes to the assembly of gut  
605 microbial communities in the zebrafish over host development. *ISME J* 10:655-664.  
606 <https://doi.org/10.1038/ismej.2015.142>

607 Carper, D. L., Carrell, A. A., Kueppers, L. M., & Frank, A. C (2018) Bacterial  
608 endophyte communities in *Pinus flexilis* are structured by host age, tissue type, and  
609 environmental factors. *Plant Soil* 428:335-352. [https://doi.org/10.1007/s11104-018-](https://doi.org/10.1007/s11104-018-3682-x)  
610 3682-x

611 Chaparro, J. M., Badri, D. V., Bakker, M. G., Sugiyama, A., Manter, D. K., & Vivanco,  
612 J. M (2013) Root exudation of phytochemicals in *Arabidopsis* follows specific patterns  
613 that are developmentally programmed and correlate with soil microbial functions. *PloS*  
614 *One* 8:e55731. <https://doi.org/10.1371/journal.pone.0055731>

615 Chaparro, J. M., Badri, D. V., & Vivanco, J. M (2014) Rhizosphere microbiome  
616 assemblage is affected by plant development. *ISME J* 8:790-803.  
617 <https://doi.org/10.1038/ismej.2013.196>

618 Compant, S., Samad, A., Faist, H., & Sessitsch, A (2019) A review on the plant  
619 microbiome: Ecology, functions, and emerging trends in microbial application. *J Adv*  
620 *Res* 19:29-37. <https://doi.org/10.1016/j.jare.2019.03.004>

621 Copeland, J. K., Yuan, L., Layeghifard, M., Wang, P. W., & Guttman, D. S (2015)  
622 Seasonal community succession of the phyllosphere microbiome. *Mol Plant Microbe*  
623 *Interact* 28:274-285. <https://doi.org/10.1094/MPMI-10-14-0331-FI>

624 Cotton, TEA., Pétriacq, P., Cameron, DD., Meselmani, MA., Schwarzenbacher, R.,  
625 Rolfe, SA., Ton, J (2019) Metabolic regulation of the maize rhizobiome by  
626 benzoxazinoids. *ISME J* 13: 1647–1658. <https://doi.org/10.1038/s41396-019-0375-2>

627 Dang, H., Zhang, T., Wang, Z., Li, G., Zhao, W., Lv, X., Zhuang, L (2021) Succession  
628 of endophytic fungi and arbuscular mycorrhizal fungi associated with the growth of  
629 plant and their correlation with secondary metabolites in the roots of plants. *BMC Plant*  
630 *Biol* 21:165. <https://doi.org/10.1186/s12870-021-02942-6>

631 Deyett, E., and Rolshausen, P.E (2020) Endophytic microbial assemblage in grapevine.  
632 *FEMS Microbiol Ecol* 96: fiae053. <https://doi.org/10.1093/femsec/fiae053>

633 Doumbou, C. L., Hamby Salove, M. K., Crawford, D. L., & Beaulieu, C (2001)  
634 Actinomycetes, promising tools to control plant diseases and to promote plant growth.  
635 *Phytoprotection* 82: 85-102. <https://doi.org/10.7202/706219ar>

636 Dries, L., Bussotti, S., Pozzi, C., Kunz, R., Schnell, S., Lohnertz, O., and Vortkamp, A  
637 (2021) Rootstocks shape their microbiome-bacterial communities in the rhizosphere of  
638 different grapevine rootstocks. *Microorganisms* 9: 822.  
639 <https://doi.org/10.3390/microorganisms9040822>

640 Elzhov, T. V., Mullen, K. M., Spiess, A., & Bolker, B (2010) Minpack. lm: R interface  
641 to the Levenberg-Marquardt nonlinear least-squares algorithm found in MINPACK.  
642 Plus support for bounds 1-2. <http://CRAN.R-project.org/package=minpack.lm>.

643 Escudié, F., Auer, L., Bernard, M., Mariadassou, M., Cauquil, L., Vidal, K., Maman,  
644 S., Hernandez-Raquet, G., Combes, S., & Pascal, G (2018) FROGS: find, rapidly,  
645 OTUs with galaxy solution. *Bioinformatics* 34:1287-1294.  
646 <https://doi.org/10.1093/bioinformatics/btx791>

647 Fox, J., & Weisberg, S (2018) An R companion to applied regression. Sage publications.

648 Govindasamy, V., Franco, C. M. M., & Gupta, V. V. S. R (2014) Endophytic  
649 actinobacteria: diversity and ecology. *Adv Endophy Res*, Springer, New Delhi 27-59.  
650 [https://doi.org/10.1007/978-81-322-1575-2\\_2](https://doi.org/10.1007/978-81-322-1575-2_2)

651 Guo, J., Ling, N., Li, Y., Li, K., Ning, H., Shen, Q., Guo, S., & Vandenkoornhuysen, P  
652 (2021) Seed-borne, endospheric and rhizospheric core microbiota as predictors of plant  
653 functional traits across rice cultivars are dominated by deterministic processes. *New*  
654 *Phytol* 230:2047-2060. <https://doi.org/10.1111/nph.17297>

655 Hardoim, P. R., Van Overbeek, L. S., Berg, G., Pirttilä, A. M., Compant, S., Campisano,  
656 A., Döring, M., & Sessitsch, A (2015) The hidden world within plants: ecological and  
657 evolutionary considerations for defining functioning of microbial endophytes.  
658 *Microbiol Mol Biol Rev* 79: 293-320. <https://doi.org/10.1128/MMBR.00050-14>

659 Hervé, M., & Hervé, M. M (2020) RVAideMemoire: testing and plotting procedures  
660 for biostatistics. The R Foundation. See [https://CRAN.R-project.org/package=](https://CRAN.R-project.org/package=RVAideMemoire)  
661 [RVAideMemoire](https://CRAN.R-project.org/package=RVAideMemoire).

662 Iannucci, A., Canfora, L., Nigro, F., De Vita, P., & Beleggia, R (2021). Relationships  
663 between root morphology, root exudate compounds and rhizosphere microbial  
664 community in durum wheat. *Appl Soil Ecol* 158:103781.  
665 <https://doi.org/10.1016/j.apsoil.2020.103781>

666 Jacoby, RP., Chen, L., Schwier, M., Koprivova, A., Kopriva, S (2020) Recent advances  
667 in the role of plant metabolites in shaping the root microbiome. *F1000Res* 9:151.  
668 <https://doi.org/10.12688/f1000research.21796.1>

669 Jumpponen, A., Jones, KL (2010) Seasonally dynamic fungal communities in the  
670 *Quercus macrocarpa* phyllosphere differ between urban and nonurban environments.  
671 *New Phytol* 186:496–513. <https://doi.org/10.1111/j.1469-8137.2010.03197.x>

672 Kaur, S., Suseela, V (2020) Unraveling arbuscular mycorrhiza-induced changes in plant  
673 primary and secondary metabolome. *Metabolites* 10:335.  
674 <https://doi.org/10.3390/metabo10080335>

675 Kiers, E. T., Duhamel, M., Beesetty, Y., Mensah, J. A., Franken, O., Verbruggen, E.,  
676 Fellbaum, C. R., Kowalchuk, G. A., Hart, M. M., & Bago, A (2011) Reciprocal rewards  
677 stabilize cooperation in the mycorrhizal symbiosis. *Science* 333:880-882.  
678 <https://doi.org/10.1126/science.1208473>

679 Legendre, P., & Gallagher, E. D (2001) Ecologically meaningful transformations for  
680 ordination of species data. *Oecologia* 129:271-280.  
681 <https://doi.org/10.1007/s004420100716>

682 Lemanceau, P., Blouin, M., Muller, D., & Moënne-Loccoz, Y (2017) Let the core  
683 microbiota be functional. *Trends Plant Sci* 22:583-595.  
684 <https://doi.org/10.1016/j.tplants.2017.04.008>

685 Lê Van, A., Quaiser, A., Duhamel, M., Michon-Coudouel, S., Dufresne, A.,  
686 Vandenkoornhuysen, P (2017) Ecophylogeny of the endospheric root fungal microbiome  
687 of co-occurring *Agrostis stolonifera*. *PeerJ* 5: e3454 <https://doi.org/10.7717/peerj.3454>

688 Lidbury, I. D. E. A., Borsetto, C., Murphy, A. R. J., Bottrill, A., Jones, A. M. E.,  
689 Bending, G. D., Hammond, J. P., Chen, Y., Wellington, E. M. H., & Scanlan, D. J (2021)  
690 Niche-adaptation in plant-associated Bacteroidetes favours specialisation in organic  
691 phosphorus mineralisation. *ISME J* 15:1040-1055. [https://doi.org/10.1038/s41396-](https://doi.org/10.1038/s41396-020-00829-2)  
692 [020-00829-2](https://doi.org/10.1038/s41396-020-00829-2)

- 693 Liu, D., & Howell, K (2021) Community succession of the grapevine fungal  
694 microbiome in the annual growth cycle. *Environ Microbiol* 23:1842-1857.  
695 <https://doi.org/10.1111/1462-2920.15172>
- 696 Mahé, S., Duhamel, M., Le Calvez, T., Guillot, L., Sarbu, L., Bretaudeau, A., Collin,  
697 O., Dufresne, A., Kiers, E. T., & Vandenkoornhuyse, P (2012) PHYMYCO-DB: a  
698 curated database for analyses of fungal diversity and evolution. *PloS One* 7:e43117.  
699 <https://doi.org/10.1371/journal.pone.0043117>
- 700 Marasco, R., Rolli, E., Fusi, M., Michoud, G., & Daffonchio, D (2018) Grapevine  
701 rootstocks shape underground bacterial microbiome and networking but not potential  
702 functionality. *Microbiome* 6:3. <https://doi.org/10.1186/s40168-017-0391-2>
- 703 Marasco, R., Alturkey, H., Fusi, M., Brandi, M., Ghiglieno, I., Valenti, L., and  
704 Daffonchio, D (2022) Rootstock-scion combination contributes to shape diversity and  
705 composition of microbial communities associated with grapevine root system. *Environ*  
706 *Microbiol* 24: 3791-3808. <https://doi.org/10.1111/1462-2920.16042>
- 707 McRose, Darcy L., Li, J., and Newman, Dianne K (2023) The chemical ecology of  
708 coumarins and phenazines affects iron acquisition by pseudomonads. *Proc Natl Acad*  
709 *Sci* 120: e2217951120. <https://doi.org/10.1073/pnas.2217951120>
- 710 Morrison-Whittle, P., & Goddard, M. R (2015) Quantifying the relative roles of  
711 selective and neutral processes in defining eukaryotic microbial communities. *ISME J*  
712 9:2003-2011. <https://doi.org/10.1038/ismej.2015.18>
- 713 Mougél, C., Offre, P., Ranjard, L., Corberand, T., Gamalero, E., Robin, C., Lemanceau,  
714 P (2006) Dynamic of the genetic structure of bacterial and fungal communities at  
715 different developmental stages of *Medicago truncatula* Gaertn. cv. Jemalong line J5.  
716 *New Phytol* 170:165–175. <https://doi.org/10.1111/j.1469-8137.2006.01650.x>
- 717 Müller, DB., Vogel, C., Bai, Y., Vorholt, JA (2016) The plant microbiota: systems-  
718 level insights and perspectives. *Annu Rev Genet* 50:211–234.  
719 <https://doi.org/10.1146/annurev-genet-120215-034952>
- 720 Ning, D., Deng, Y., Tiedje James, M., & Zhou, J (2019) A general framework for  
721 quantitatively assessing ecological stochasticity. *Proc Natl Acad Sci USA* 116:16892-  
722 16898. <https://doi.org/10.1073/pnas.1904623116>
- 723 Pérez-Jaramillo, J. E., Carrión, V. J., Bosse, M., Ferrão, L. F. V., De Hollander, M.,  
724 Garcia, A. A. F., Ramírez, C. A., Mendes, R., & Raaijmakers, J. M (2017) Linking  
725 rhizosphere microbiome composition of wild and domesticated *Phaseolus vulgaris* to  
726 genotypic and root phenotypic traits. *ISME J* 11:2244-2257.  
727 <https://doi.org/10.1038/ismej.2017.85>
- 728 Porrás-Alfaro, A., & Bayman, P (2011) Hidden fungi, emergent properties: endophytes  
729 and microbiomes. *Annu Rev Phytopathol* 49:291-315. <https://doi.org/10.1146/annurev-phyto-080508-081831>
- 731 Quast, C., Pruesse, E., Yilmaz, P., Gerken, J., Schweer, T., Yarza, P., Peplies, J., &  
732 Glöckner, F. O (2012) The SILVA ribosomal RNA gene database project: improved  
733 data processing and web-based tools. *Nucleic Acids Res* 41: D590-D596.  
734 <https://doi.org/10.1093/nar/gks1219>
- 735 Renouf, V., Claisse, O., and Lonvaud-Funel, A (2005) Understanding the microbial  
736 ecosystem on the grape berry surface through numeration and identification of yeast

- 737 and bacteria. *Austral J Grape Wine Res* 11: 316-327. <https://doi.org/10.1111/j.1755->  
738 0238.2005.tb00031.x
- 739 Saleem, M., Law, A. D., Sahib, M. R., Pervaiz, Z. H., & Zhang, Q (2018) Impact of  
740 root system architecture on rhizosphere and root microbiome. *Rhizosphere* 6:47-51.  
741 <https://doi.org/10.1016/j.rhisph.2018.02.003>
- 742 Schrey, S. D., & Tarkka, M. T (2008) Friends and foes: streptomycetes as modulators  
743 of plant disease and symbiosis. *Antonie Van Leeuwenhoek* 94:11-19.  
744 <https://doi.org/10.1007/s10482-008-9241-3>
- 745 Searle, S. R., Speed, F. M., & Milliken, G. A (1980) Population marginal means in the  
746 linear model: an alternative to least squares means. *Am Stat* 34:216-221.  
747 <https://doi.org/10.1080/00031305.1980.10483031>
- 748 Sloan, W. T., Lunn, M., Woodcock, S., Head, I. M., Nee, S., & Curtis, T. P (2006)  
749 Quantifying the roles of immigration and chance in shaping prokaryote community  
750 structure. *Environ Microbiol* 8:732-740. <https://doi.org/10.1111/j.1462->  
751 2920.2005.00956.x
- 752 Smith, S. E., Read, D. J (2010) *Mycorrhizal symbiosis*. Academic Press (Third edition).  
753 <https://doi.org/10.1097/00010694-198403000-00011>
- 754 Swift, J.F., Hall, M.E., Harris, Z.N., Kwasniewski, M.T., and Miller, A.J (2021)  
755 Grapevine microbiota reflect diversity among compartments and complex interactions  
756 within and among root and shoot systems. *Microorganisms* 9: 92.  
757 <https://doi.org/10.3390/microorganisms9010092>
- 758 Trivedi, P., Leach, J. E., Tringe, S. G., Sa, T., Singh, B. K (2020) Plant-microbiome  
759 interactions: from community assembly to plant health. *Nat Rev Microbiol* 18:607-621.  
760 <https://doi.org/10.1038/s41579-020-0412-1>
- 761 Vandenkoornhuyse, P., Husband, R., Daniell, T. J., Watson, I. J., Duck, J. M., Fitter, A.  
762 H., Young, J. P. W (2002) Arbuscular mycorrhizal community composition associated  
763 with two plant species in a grassland ecosystem. *Mol Ecol* 11:1555-1564. <https://>  
764 [doi.org/10.1046/j.1365-294x.2002.01538.x](https://doi.org/10.1046/j.1365-294x.2002.01538.x)
- 765 Vandenkoornhuyse, P., Quaiser, A., Duhamel, M., Le Van, A., Dufresne, A (2015) The  
766 importance of the microbiome of the plant holobiont. *New Phytol* 206:1196-1206.  
767 <https://doi.org/10.1111/nph.13312>
- 768 Vannier, N., Mony, C., Bittebière, A.-K., & Vandenkoornhuyse, P (2015) Epigenetic  
769 mechanisms and microbiota as a toolbox for plant phenotypic adjustment to  
770 environment. *Front Plant Sci* 6:1159. <https://doi.org/10.3389/fpls.2015.01159>
- 771 Vannier, N., Mony, C., Bittebière, A.-K., Michon-Coudouel, S., Biget, M., &  
772 Vandenkoornhuyse, P (2018) A microorganisms' journey between plant generations.  
773 *Microbiome* 6:79. <https://doi.org/10.1186/s40168-018-0459-7>
- 774 Venkataraman, A., Bassis, CM., Beck, JM., Young, VB., Curtis, JL., Huffnagle, GB,  
775 Schmidt, TM (2015) Application of a neutral community model to assess structuring of  
776 the human lung microbiome. *mBio* 6:e02284-14. <https://doi.org/10.1128/mBio.02284->  
777 14
- 778 Vink, S.N., Dini-Andreote, F., Höfle, R., Kicherer, A., and Salles, J.F (2021) Interactive  
779 effects of scion and rootstock genotypes on the root microbiome of grapevines (*Vitis*  
780 spp. L.). *Appl Sci* 11:1615. <https://doi.org/10.3390/app11041615>

- 781 Vives-Peris, V., de Ollas, C., Gómez-Cadenas, A., Pérez-Clemente, RM (2020) Root  
782 exudates: from plant to rhizosphere and beyond. *Plant Cell Rep* 39:3–17.  
783 <https://doi.org/10.1007/s00299-019-02447-5>
- 784 Voges, MJEEE., Bai., Y, Schulze-Lefert, P., Sattely, ES (2019) Plant-derived  
785 coumarins shape the composition of an Arabidopsis synthetic root microbiome. *Proc*  
786 *Natl Acad Sci USA* 116:12558–12565. <https://doi.org/10.1073/pnas.1820691116>
- 787 Werner, G. D. A., & Kiers, E. T (2015) Order of arrival structures arbuscular  
788 mycorrhizal colonization of plants. *New Phytol* 205:1515-1524.  
789 <https://doi.org/10.1111/nph.13092>
- 790 Xiong, C., Zhu, Y. G., Wang, J. T., Singh, B., Han, L. L., Shen, J. P., Li, P. P., Wang,  
791 G. B., Wu, C. F., Ge, A. H (2021) Plant developmental stage drives the differentiation  
792 in ecological role of the maize microbiome. *Microbiome* 9:171.  
793 <https://doi.org/10.1186/s40168-021-01118-6>
- 794 Yang, T., Chen, Y., Wang, X.-X., & Dai, C.-C (2013) Plant symbionts: keys to the  
795 phytosphere. *Symbiosis* 59:1-14. <https://doi.org/10.1007/s13199-012-0190-2>
- 796 Zarraindia, I., Owens, S. M., Weisenhorn, P., West, K., Hampton-Marcell, J., Lax,  
797 S., Bokulich, N. A., Mills, D. A., Martin, G., & Taghavi, S (2015) The soil microbiome  
798 influences grapevine-associated microbiota. *mBio* 6:e02527-02514.  
799 <https://doi.org/10.1128/mBio.02527-14>
- 800 Zhalnina, K., Louie, K. B., Hao, Z., Mansoori, N., da Rocha, U. N., Shi, S., Cho, H.,  
801 Karaoz, U., Loqué, D., & Bowen, B. P (2018) Dynamic root exudate chemistry and  
802 microbial substrate preferences drive patterns in rhizosphere microbial community  
803 assembly. *Nat Microbiol* 3:470-480. <https://doi.org/10.1038/s41564-018-0129-3>
- 804 Zhang, J., Wang, E. T., Singh, R. P., Guo, C., Shang, Y., Chen, J., & Liu, C (2019)  
805 Grape berry surface bacterial microbiome: impact from the varieties and clones in the  
806 same vineyard from central China. *J Appl Microbiol* 126:204-214.  
807 <https://doi.org/10.1111/jam.14124>



808 **Statements and Declarations**

809 **Funding**

810 This work was supported by a grant from the CNRS-EC2CO program (HOLOBIONT  
811 project), CNRS-IRP program (M-AGRI project) and by the "Agence Nationale de la  
812 Recherche et de la Technologie" (ANRT) through an industrial CIFRE agreement  
813 between Château Palmer, Château Latour, Sovivins, Pépinière de Salettes and the  
814 University of Rennes 1 (Agreement N° 2017/1579).

815 **Competing interests**

816 The authors declared no conflicts of interest.

817 **Author contribution**

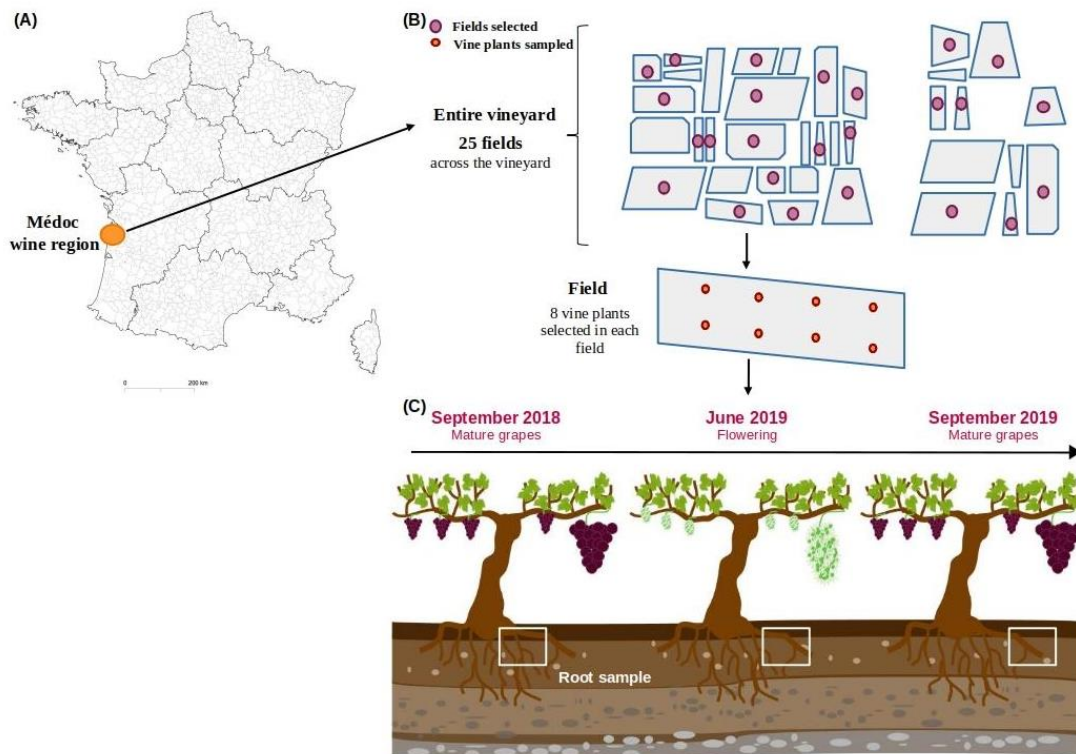
818 MB, CM, SP, VC and PV conceived the project. PV, CM and MB set up the  
819 methodology of the study. MB, CM, OJ, NL and PV conducted the sampling. MB  
820 conducted lab experiments with the help of AM. RCV and SMC performed the  
821 sequencing and MB and TW analyzed the sequence data. MB and TW performed the  
822 statistical analyses with advice from CM, MH and NL. MB wrote the first draft of the  
823 paper. All the authors gave their final approval for publication.

824 **Data Accessibility**

825 Data are available on Figshare <https://figshare.com/s/6c6ca1fee254f88e0598>.

826 Sequence data are available at European Nucleotide Archive (ENA) under accession  
827 number PRJEB47615.

828 **Figures**



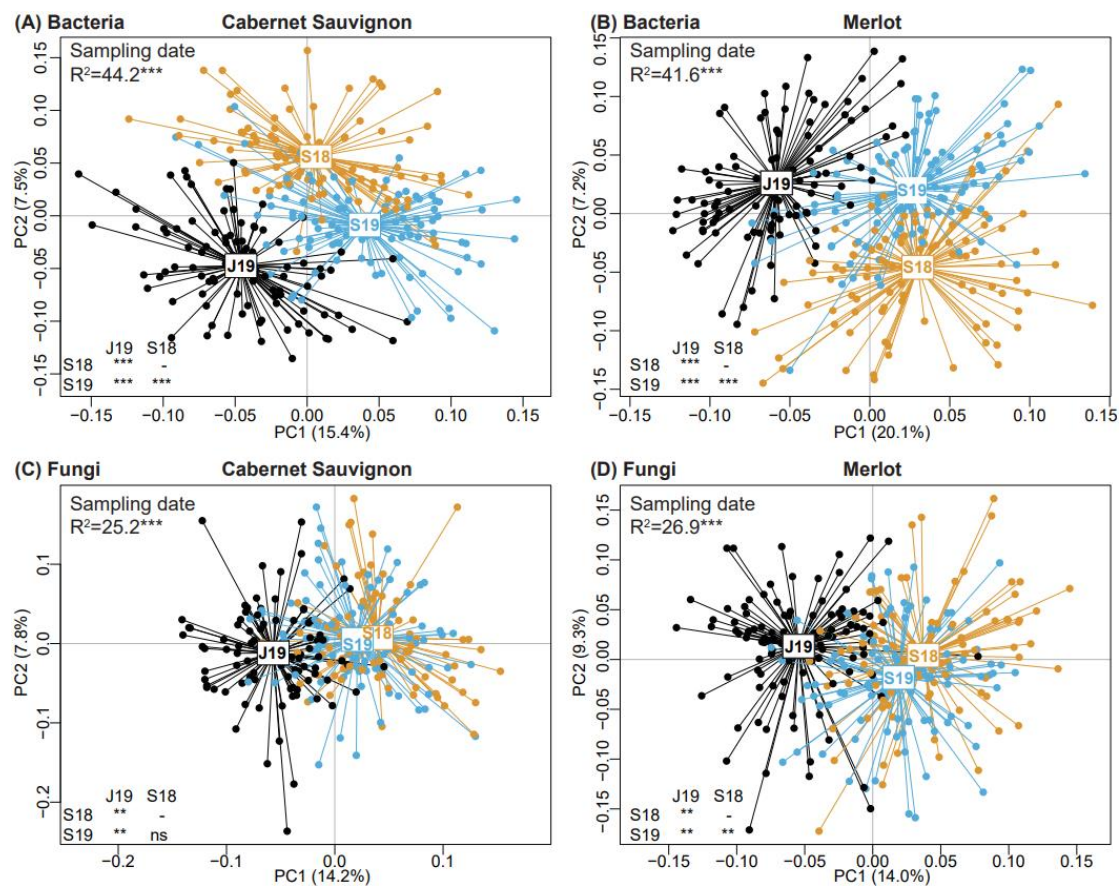
829

830 **Fig.1 Experimental design and sampling scheme.**

831 (A) Map of the study site located near Bordeaux (France) in the Medoc wine region.

832 (B) Scheme representing the nearby location of the 25 fields across the vineyard and  
833 the 8 equidistant grapevines sampled in each field.

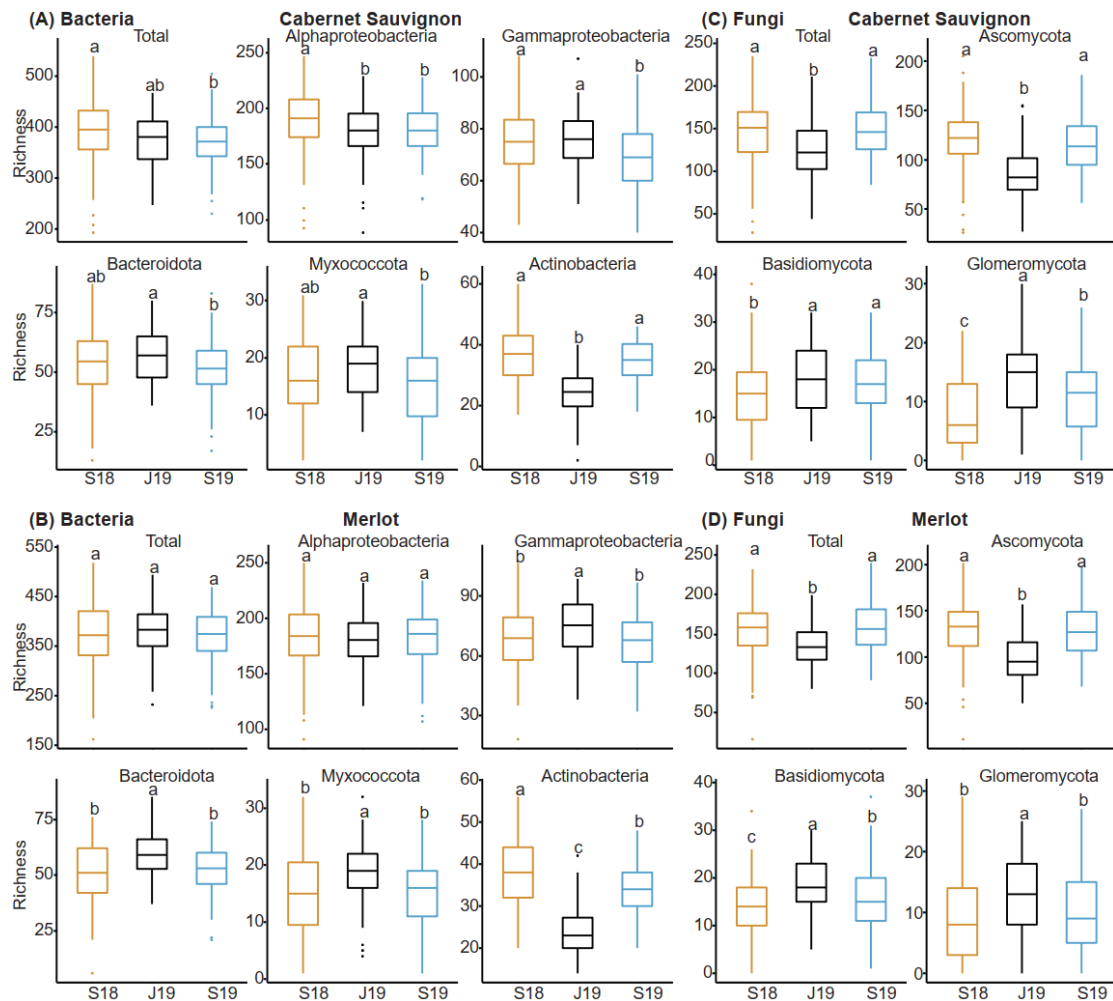
834 (C) Sampling dates of root collection associated with plant developmental stage:  
835 September 2018 and 2019 (S18/S19 - mature grapes) and June 2019 (J19 - flowering  
836 period).



837

838 **Fig. 2 Principal coordinate analysis (PCoA) plots depicted the differences of the**  
 839 **microbial communities.**

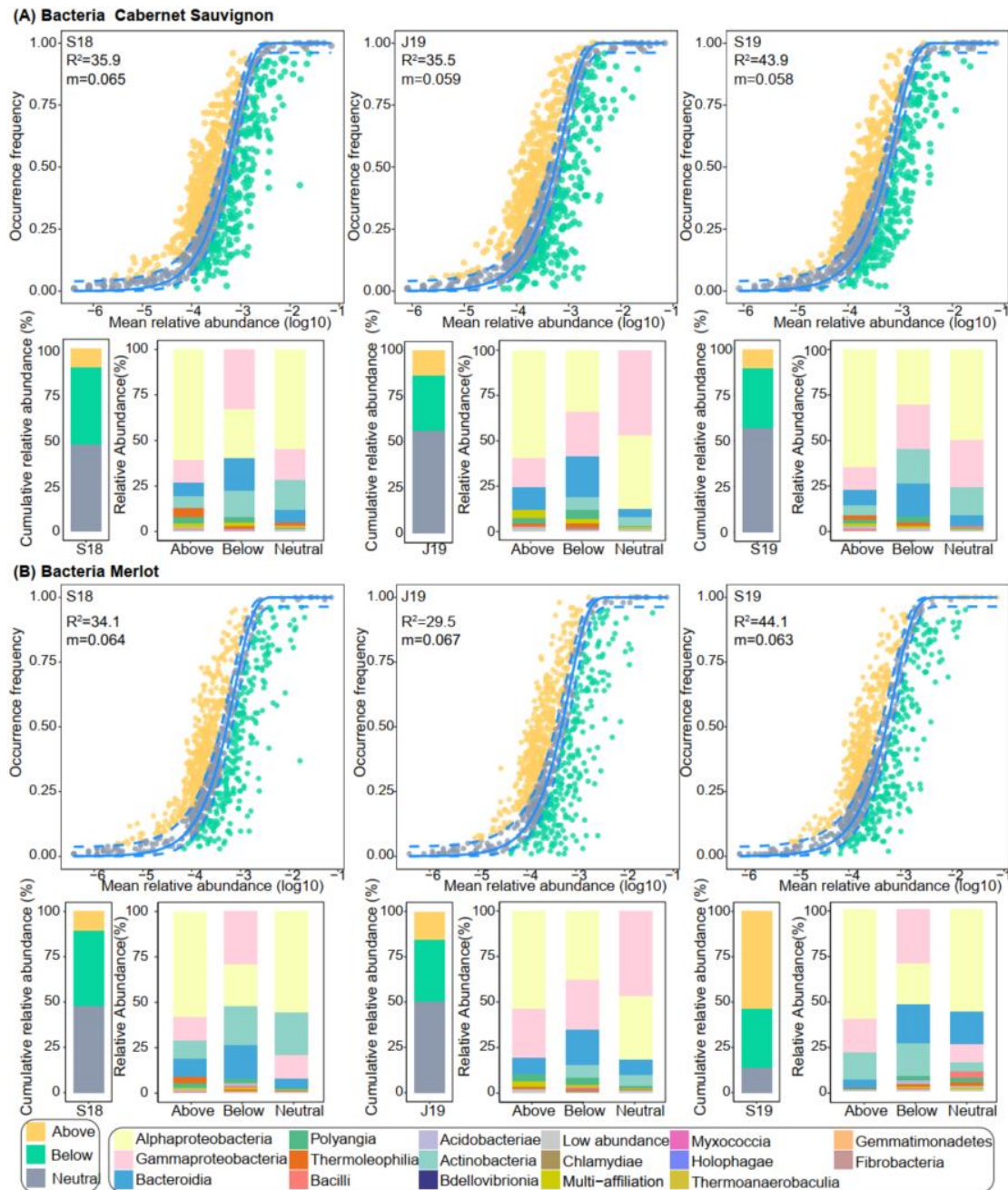
840 Analyses were done on the sequence-cluster matrix of the bacterial (A, B) and fungal  
 841 (C, D) communities and for the two cultivars considered: the Cabernet-Sauvignon (A,  
 842 C) and the Merlot (B, D). Results from the permutation tests testing the effect of the  
 843 sampling dates (\*\*\*:  $p < 0.001$ ) and  $R^2$ , percentage of variance explained, are included  
 844 on the plots. Statistical results from the pairwise comparisons are also described on the  
 845 plots (\*\*:  $p < 0.01$ ; \*\*\*:  $p < 0.001$ ; ns:  $p > 0.05$ ). S18-yellow: September 2018; J19-black:  
 846 June 2019 and S19-blue: September 2019.



847

848 **Fig. 3 Effect of the sampling date on bacterial and fungal sequence-cluster richness**  
 849 **at the  $\alpha$ -diversity scale.**

850 Linear mixed models for each sampling campaign were used to test whether the  
 851 sampling date influenced microbial richness (grapevine individual considered as  
 852 random effect). (A), (B) Results of bacterial communities for Cabernet-Sauvignon and  
 853 Merlot cultivars respectively. (C), (D) Results of fungal communities for the Cabernet-  
 854 Sauvignon and the Merlot cultivars respectively. S18-yellow: September 2018; J19-  
 855 black: June 2019 and S19-blue: September 2019.

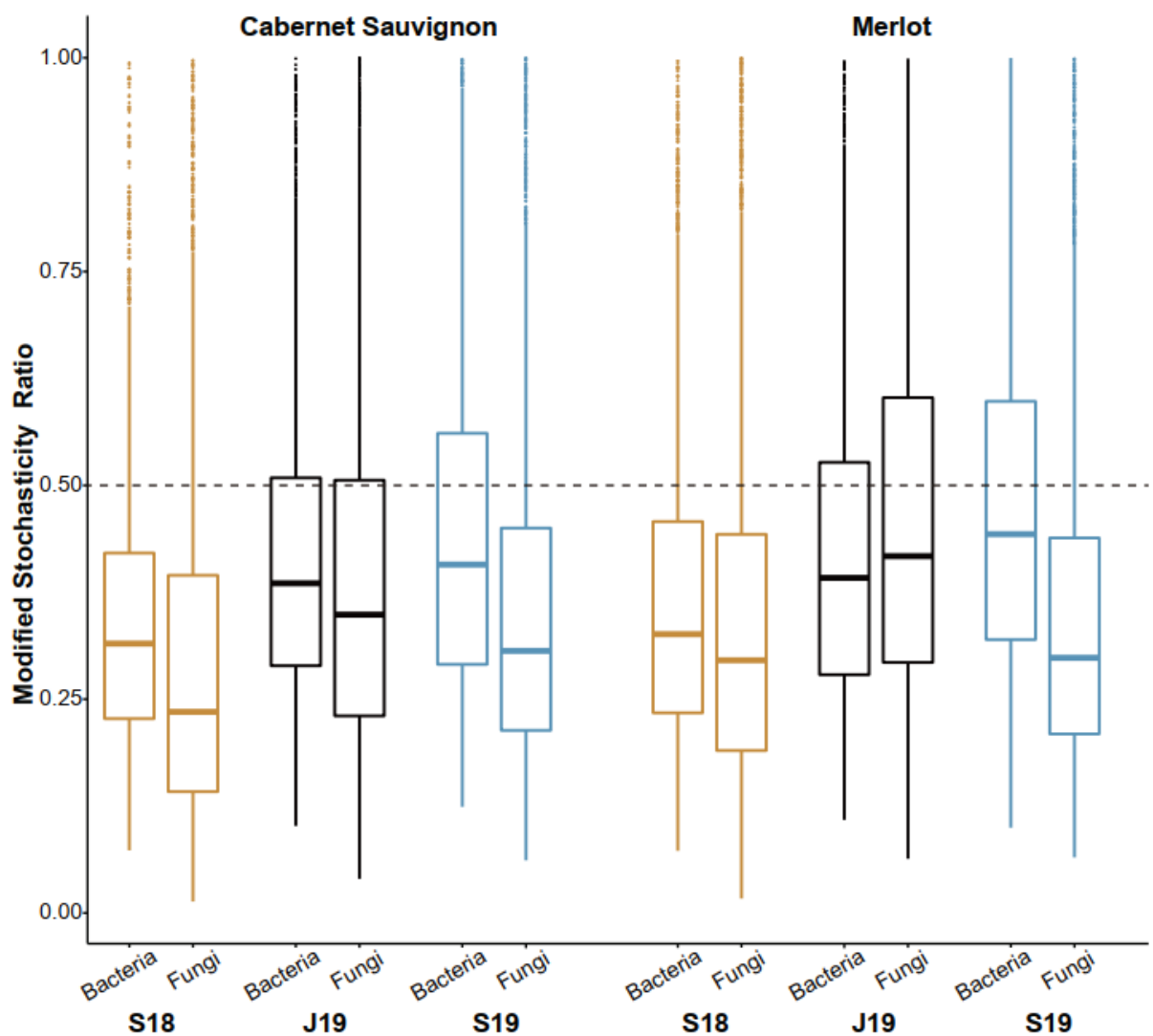


856

857 **Fig. 4 Partition of deterministic and ecologically neutral processes of bacterial**  
 858 **community assembly using neutral community model (NCM).**

859 (A) S18/J19/S19-Cabernet-Sauvignon and (B) S18/J19/S19-Merlot, served as the  
 860 community source to create neutral models. The first graphs showed the occurrence  
 861 frequencies predicted through the NCM. The sequence-clusters occurring more  
 862 frequently than expected were dotted in yellow while the ones occurring less frequently

863 were colored in green. The solid blue line indicates the best fit of the model and the  
864 dashed ones indicate 95% confidence intervals. The dashed lines indicate the envelope  
865 of neutrally. “m” (estimate rate) and  $R^2$  ( $0 < R^2 \leq 1$ , adequacy of the model fitting) are  
866 indicated on the graphs. The single bar charts indicated cumulative sequence-clusters  
867 occurrence frequencies of Above, Neutral and Below partitions; the combined bar  
868 charts represent ranked cumulative relative abundance of taxonomic groups of the three  
869 sequence-cluster partitions



870

871 **Fig. 5 Modified normalized stochasticity ratios (MST) estimated to measure the**  
872 **relative importance of deterministic processes of assembly.**

873 Bar plots showed the bacterial and fungal MST values under different treatments. S18-  
874 yellow: September 2018; J19-black: June 2019 and S19-blue: September 2019.